Expression of Na^+-dependent citrate transport in a strongly metastatic human prostate cancer PC-3M cell line: regulation by voltage-gated Na^+ channel activity

Maria E. Mycielska[1], Christopher P. Palmer, William J. Brackenbury and Mustafa B. A. Djamgoz

[1]*Department of Biological Sciences, Neuroscience Solutions to Cancer Research Group, Sir Alexander Fleming Building, Imperial College London, South Kensington Campus, London SW7 2AZ, UK*

Prostate is a unique organ which synthesizes and releases large amounts of citrate. It has been shown that in metastatic prostate cancer, the amount of citrate in prostatic fluid is significantly reduced, approaching the level normally found in blood. In our previous study, we characterized electrophysiologically the mechanism of citrate transport in a normal prostatic epithelial (PNT2-C2) cell line. It was concluded that the cells expressed a novel transporter carrying 1 citrate^{3-} together with 4 K^+, primarily out of cells. In the present study, we aimed similarly to characterize the mechanism(s) of citrate transport in a strongly metastatic human prostate cancer (PC-3M) cell line and to compare this with the previous data. Citrate transport in PC-3M cells was found to be both Na^+ and K^+ dependent. Intracellular application of citrate produced an outward current that was primarily K^+ dependent whilst extracellular citrate elicited an inward current that was mainly Na^+ dependent. The electrophysiological and pharmacological characteristics of the citrate outward current were similar to the K^+-dependent citrate transporter found in the PNT2-C2 cells. On the other hand, the inward citrate current had a markedly different reversal potential, ionic characteristics, inhibitor profile and pH sensitivity. Preincubation of the PC-3M cells (24 or 48 h) with the voltage-gated Na^+ channel (VGSC) blocker tetrodotoxin (TTX) significantly reduced the Na^+ sensitivity of the citrate current, up-regulated VGSC mRNA expression but did not change the partial permeability of the membrane to Na^+. It was concluded (a) that PC-3M cells express a K^+-dependent transporter (carrying citrate outward), similar to that found in normal prostate epithelial cells, as well as (b) a Na^+-dependent transporter (carrying citrate inward). The molecular nature of the latter was investigated by RT-PCR; the three known Na^+-dependent citrate/dicarboxylate transporters could not be detected. VGSC activity, which itself has been associated with metastatic prostate cancer, had a differential effect on the two citrate transporters, down-regulating the expression of the Na^+-dependent component whilst enhancing the K^+-dependent citrate transporter.

(Resubmitted 18 November 2004; accepted 16 December 2004; first published online 20 December 2004)
Corresponding author M. E. Mycielska: Department of Biological Sciences, Sir Alexander Fleming Building, Imperial College London, South Kensington Campus, London SW7 2AZ, UK. Email: m.mycielska@imperial.ac.uk

Prostate is a unique mammalian organ which produces and releases large amounts of citrate (Costello & Franklin, 1991). This is possible because the rate-limiting enzyme, m-aconitase, expressed in prostate epithelial cells, is inhibited by the high levels of intracellular Zn^{2+} present (Costello *et al.* 2000*a*). In turn, expression of m-aconitase is regulated transcriptionally by testosteron and prolactin (Costello & Franklin, 1991). It has been shown recently that Zn^{2+} is transported into prostatic cells by the Zn^{2+} transporter hZIP1 present in the plasma membrane (Franklin *et al.* 2003).

In a previous study, we have shown that normal human prostate epithelial PNT2-C2 cells possess a citrate transporter which was some four times more efficient in transporting citrate outward than inward (Mycielska & Djamgoz, 2004). The transporter had higher affinity for the trivalent form of the citrate which would be present at $pH > 7$ (Mycielska & Djamgoz, 2004). Importantly, citrate was coupled to co-transport of K^+ in a stoichiometry of 1 : 4 (citrate : K^+). No Na^+-dependent citrate current could be detected in these cells (Mycielska & Djamgoz, 2004).

 DOI: 10.1113/jphysiol.2004.079491

Whilst citrate occurs in normal prostate in large amounts ($\sim 13 \times 10^3$ nM (g wet weight)$^{-1}$), the level drops significantly in prostate cancer ($1–3 \times 10^3$ nM (g wet weight)$^{-1}$) and almost disappears when cancer becomes metastatic (< 500 nM (g wet weight)$^{-1}$). In fact, reduction of the citrate level has been suggested to be necessary for the cells to acquire metastatic behaviour (Costello *et al.* 1999*a*). However, it is not known whether this reduction results from a defect in citrate production (e.g. due to a lack of Zn^{2+}) or/and it involves a change in citrate transportation (Liang *et al.* 1999; Feng *et al.* 2003). Changes in monocarboxylate transporter expressions have been related to the acquisition of metastatic behaviour in some human cancers (Miyauchi *et al.* 2004; Coady *et al.* 2004). Na^+-coupled monocarboxylate transport, which is responsible for growth inhibition, has been shown to be silenced by methylation and this is considered to occur early in the metastatic process (Li *et al.* 2003).

The main aim of this study was to investigate the mechanism of citrate transport in a strongly metastatic (PC-3M) cell line of human prostate cancer and compare this with the previously characterized K^+-dependent citrate transporter found in normal human prostate epithelial PNT2-C2 cells (Mycielska & Djamgoz, 2004).

Methods

Cell culture

Experiments were carried out on human prostate cancer PC-3M cells. This is a strongly metastatic cell line derived originally from a liver metastasis of human prostate cancer (Chu *et al.* 2001). The PC-3M cells were grown in Roswell Park Memorial Institute (RPMI-1640) medium, supplemented with 10% fetal calf serum, 4 mM L-glutamine, 1 g l^{-1} sodium bicarbonate, 4.5 g l^{-1} glucose and 1 mM sodium pyruvate in 10 cm Petri dishes maintained in a humidified incubator with 5% CO_2 at 37°C. The normal prostate cells, PNT2-C2, were grown as previously described (Mycielska & Djamgoz, 2004). Three days before the patch-clamp recordings, the cells were re-plated into 35 mm Petri dishes at a density of 5×10^4 per dish.

Electrophysiology

The electrophysiological procedures and solutions were as previously described (Mycielska & Djamgoz, 2004). Briefly, prior to patch-clamp recording, the growth medium was replaced with an external bath (EB) solution containing (mM): NaCl (118), $NaHCO_3$ (26), KCl (5.4), $MgCl_2$ (1), $CaCl_2$ (2.5), D-glucose (5.6) and Hepes (5), pH = 7.2, adjusted with 1 M NaOH or 1 mM HCl. Patch pipettes were filled with a solution containing (mM): NaCl (5), KCl (145), $MgCl_2$ (2), $CaCl_2$ (1), Hepes (10) and EGTA (11), pH = 7.4, adjusted with 1 M KOH (tip resistances, 5–15 MΩ). Whole-cell membrane currents were recorded from single cells using an Axopatch 200B amplifier (Axon Instruments, Foster City, CA, USA). Analog signals were filtered using a low-pass (5 kHz) Bessel filter (Axon Instruments). Signals were sampled at 50 kHz and digitized using a Digidata (1200) interface. Data acquisition and analysis were performed using pClamp (Axon Instruments) software. The holding potential was −45 mV, unless stated otherwise.

Citrate was dialysed into the cells, in the whole-cell recording mode, by including 0.1 mM Na^+- or K^+-citrate salt in the patch pipette solution. The same procedure was used for intracellular application of other compounds or Krebs cycle intermediates.

Enzyme spectrophotometry

Cellular uptake and release of citrate were measured by the spectrophotometric 'citrate lyase method' described earlier (Petrarulo *et al.* 1995; Mycielska & Djamgoz, 2004). For the uptake as well as the release experiments, PC-3M cells were plated in 96-well dishes at a density of 2×10^4 cm^{-2} and grown for 3 days. In the case of uptake, prior to experiments, the cells were washed carefully and then incubated with 10 mM Na^+-citrate for 30 min. After thorough washing with normal EB solution, the cells were digested in RIPA buffer (50 μl well^{-1}). The citrate content of the buffer, containing the cellular uptake, was determined as before (Petrarulo *et al.* 1995; Mycielska & Djamgoz, 2004). Absorption in the medium at 330 nm was measured and subtracted from the reading obtained after adding citrate lyase to the cuvettes. In the case of the release experiments, the cells were washed carefully and incubated in EB solution containing 10 mM Na^+-citrate for 30 min. Then, the cells were washed carefully and left in 50 μl well^{-1} EB solution (normal or modified ionic content) for 5–60 min. Supernatant was collected and citrate content determined as previously (Petrarulo *et al.* 1995; Mycielska & Djamgoz, 2004). Data from these measurements are presented as 'absorbance' which was directly proportional to the concentration of citrate present (Petrarulo *et al.* 1995). Absorbancies in all EB solutions used measured before exposure to cells were insignificant.

Pharmacological agents

The following pharmacological agents were tested for their effect on citrate transport: phloretin, diethyl pyrocarbonate (DEPC), dinitrophenol (DNP), *N*,*N*,*N*′,*N*′-tetrakis (2-pyridylmethyl) etylenediaminepentaethylene (TPEN), ouabain, LiCl, amiloride, 4-aminopyridine (4-AP), anthracene-9-carboxylic acid

(9-AC), lonidamine and SCH28080. All of these were purchased from Sigma (Dorset, UK) except 9-AC, lonidamine and SCH28080 which were purchased from Tocris Cookson (Bristol, UK), and tetrodotoxin (TTX) which was purchased from Alomone (Towcester, UK).

Ionic substitutions

The solutions used in ionic substitution experiments were also as before (Mycielska & Djamgoz, 2004). Essential details are given in the respective figure legends. Effects of different ions on citrate transport were studied by applying extracellular solutions with modified ionic content whilst (a) dialysing the cells with intracellular citrate in steady state or (b) pulsing the cells with extracellular citrate (10 mM). Any effect was compared with control data obtained from experiments performed on cells patched with normal intracellular pipette solution for (a), or without extracellular citrate for (b), respectively.

Stoichiometry

The stoichiometry of the Na^+ dependence of inward citrate transport (assumed to be mainly Na^+ dependent – see later) was studied as described earlier (Chen *et al.* 1998; Mycielska & Djamgoz, 2004).

Conventional RT-PCR study of citrate transporter mRNA expression

Total RNA was isolated from PNT2-C2 and PC-3M cells using a Qiagene RNAeasy kit. The integrity of the RNA used for cDNA synthesis was examined by visual inspection for the presence of intact 18 s and 28 s ribosomal RNAs upon agarose gel electrophoresis. The quantity and purity of total RNA was tested by spectrophotometry at 260/280 nm. The RNA used for cDNA synthesis was treated with DNase I. One microgram of RNA was primed using random hexamers and reverse transcribed using a Superscript II reverse transcription kit (Invitrogen) as described by the manufacturer. Human liver and kidney cDNAs were obtained from Biochain (USA). Each PCR reaction was performed in a 25 μl volume with a JumpStart AccuTaq LA Taq DNA polymerase kit (Sigma) and contained 0.4 μM of each primer and 0.5 μl of cDNA, as described by the manufacturer. PCR utilized the following thermocycles: 94°C × 2 min, 1 cycle; 94°C × 30 s, 55°C × 30 s, 68°C × 30 s, 35 cycles; 68°C × 5 min, 1 cycle. The following primers were utilized for the detection of the three known citrate transporter (plus a splice variant) mRNAs:

(1) NaDC1: 5′-CAATGCCATCGTCTTCTCTT-3′ and 5′-TGGTGTTGGCCAGGCTTGGC-3′;

(2) NaDC1 (alternative splice form, accession number AA603049): 5′-TTAACAGCCCAGAGGCTGTT-3′ and 5′-TGCATGCACATGATCCTAGG-3′;

(3) NaDC3: 5′-GCCTCTGGACACTTGCTGGT-3′ and 5′-GTCCGAAATGTGTCATTGGC-3′;

(4) NaCT: 5′-TTGCCTTCATGTTGCCTGTG-3′ and 5′-CTCAATATGTGTCACATTAG-3′.

The quality of cDNAs was verified using primers to β-actin (Biochain). PCR reactions were separated by 1.5% agarose gel electrophoresis and visualized by ethidium bromide staining.

Real-time PCR measurement of Nav1.7 mRNA expression

Total RNA was extracted from 35 mm dishes of PC-3M cells using StrataPrep Absolutely RNA Miniprep kits (Stratagene, La Jolla, CA, USA). Approximate RNA quantity was visualized by spectrophotometric absorbance at 260 nm. For each sample, 1 μg of RNA was reverse-transcribed into cDNA with Superscript II reverse-transcriptase (Invitrogen, Paisley, UK), using 250 ng of random hexamer mix (Amersham Biosciences, Chalfont, UK) as a primer. Each cDNA synthesis was performed in a total volume of 20 μl, which was diluted to 100 μl with H_2O at the end of the reaction and stored at −20°C for subsequent analysis. Real-time PCR was performed using the DNA Engine Opticon 2 system (MJ Research, Waltham, MA, USA). Triplicate PCR reactions were run for each sample and β-actin was measured as a control/reference gene to normalize the respective measured Nav1.7 expression. PCR reactions were performed in a total reaction volume of 20 μl, containing 10 μl Quantitect SYBR Green PCR mix (Qiagen, Crawley, UK), 500 nM of each specific primer and 5 μl of cDNA. The PCR was run with an initial step of 95°C for 15 min to activate the HotStar Taq, followed by 40 cycles of 95°C for 30 s, 59 or 67°C (depending on primer pair) for 30 s and 72°C for 30 s. Fluorescence from incorporation of SYBR green to double stranded DNA was measured after each cycle. A no-template control was included for each PCR. Product composition was verified with a melt curve in 0.3°C steps from 65°C to 95°C. A standard calibration curve was included for Nav1.7 and β-actin, using five serial dilutions of control-treated PC-3M cDNA covering a range of four orders of magnitude.

The Nav1.7 primers were: 5′- TATGACCATGAATA ACCCGC-3′ and 5′-TCAGGTTTCCCATGAACAGC-3′; annealing temperature was 59°C (Diss *et al.* 2001). The β-actin primers were: 5′-AGCCTCGCCTTTGCCGA-3′ and 5′-CTGGTGCCTGGGGCG-3′; annealing temperature was 67°C (Kreuzer *et al.* 1999).

The threshold amplification cycles (C_Ts) were determined using the Opticon Monitor 2 software and

then analysed by the $2^{-\Delta\Delta CT}$ method (Livak & Schmittgen, 2001). The relative expression of Nav1.7 was determined in PC-3M cells treated with TTX (1 μM; 24 and 48 h) and compared with untreated control cells, for three separate treatments. Input cDNA was normalized using the reference gene β-actin.

Data analysis

Data were analysed as means ± S.E.M. Change in membrane current is indicated as 'Δ', expressed as either a percentage change, defined as follows:

$$\Delta I_i = [(I_i - I_o)I_o] \times 100\,(\%)$$

or an absolute difference, where I_i is the current generated in a modified experimental condition and I_o is the control value of the current. In the text, '*n*' refers to the number of experiments, each on a different cell. Statistical significance was determined using Student's *t* test.

Results

Basic ionic characteristics of PC-3M cells

PC-3M cells had a resting membrane potential of -52.3 ± 6.1 mV ($n = 14$). The cells were sensitive to changes in extracellular Na^+, K^+ and Cl^- concentrations, but not sensitive to Mg^{2+}. Application of low-Na^+ (37.8 and 26 mM; choline-substituted) EB solutions produced an outward current (I_{Na}) of 29.5 ± 5.0 and 39.9 ± 4.0 pA, respectively ($n = 10$). These changes were sensitive to TTX (1 μM), which reduced I_{Na} significantly by $25.0 \pm 8.2\%$ ($P = 0.003$; $n = 9$). Application of high-K^+ (54 and 118 mM; Na^+-substituted) EB solutions resulted in inward currents of -25.2 ± 5.0 and -39.7 ± 3.8 pA, respectively ($n = 10$). The K^+ channel blocker 4-AP (5 mM) generated an inward current of 9.0 ± 2.0 pA ($n = 11$). Lowering the extracellular Cl^- concentration 10-fold (gluconate-substituted) resulted in an outward current of 121.1 ± 15.3 pA ($n = 8$). From these measurements, it was concluded that PC-3M cells had significant resting permeability for K^+, Na^+ and Cl^-.

Membrane currents induced by citrate

At the −45 mV holding potential, the membrane current was very stable (Fig. 1*A*, lower trace). In contrast, in recordings made with a patch pipette containing 0.1 mM Na^+-citrate salt, an outward current ($I_{ci,out}$) developed gradually (Fig. 1*A*, upper trace), reaching (by 53.0 ± 7.6 s) a stable plateau of 69.6 ± 7.5 pA ($n = 10$). Equimolar NaCl induced only a small outward current of 18.2 ± 5.1 pA ($n = 13$).

Application of extracellular citrate caused a faster, inward current ($I_{ci,in}$) (Fig. 1*B*). Extracellular (10 mM) Na^+-citrate resulted in an inward current of -52.1 ± 7.2 pA ($n = 32$). This current was sustained and no desensitization was seen even when citrate was applied repeatedly to the same cell (tested up to 5 times).

Dose dependencies

The dose dependence of $I_{ci,out}$ was tested in the concentration range 0.01–10 mM intracellular Na^+-citrate (Fig. 1*C*). The current was dose dependent up to 1 mM; further increase in the citrate concentration to 10 mM

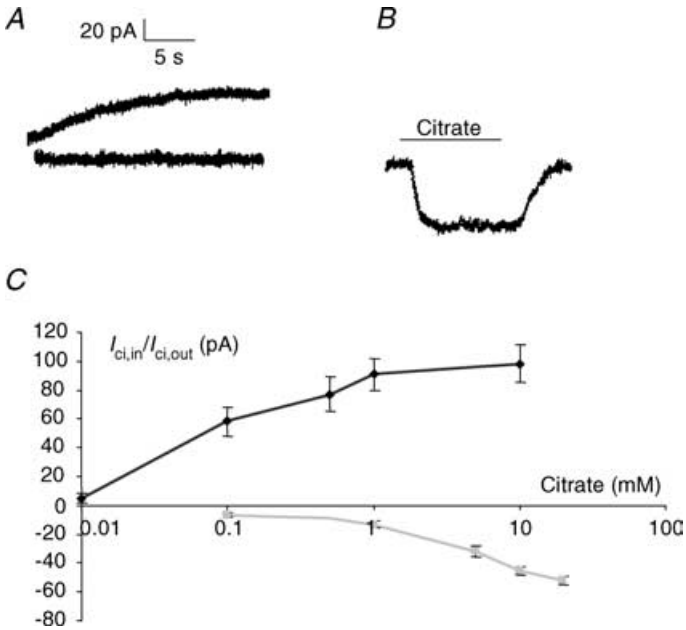

Figure 1. Citrate-induced membrane currents in PC-3M cells
A, membrane currents recorded from two different cells immediately after breaking the membrane in the whole-cell recording mode with a pipette containing 0.1 mM Na^+-citrate (upper-most trace) and with a pipette filled with normal solution, i.e. containing no citrate (lower trace). Holding potentials, –45 mV. *B*, membrane current obtained from a single cell in response to extracellular application of 10 mM Na^+-citrate. *C*, dose–response relationship of $I_{ci,out}$ (black diamonds) and $I_{ci,in}$ (grey squares). For $I_{ci,out}$, the following concentrations of Na^+-citrate were dialysed into cells: 0.01, 0.1, 0.5, 1 and 10 mM, and the corresponding outward currents were measured in steady state. For $I_{ci,in}$, extracellular citrate was used at the following concentrations: 0.1, 1, 5, 10 and 20 mM. Each point represents the mean ± S.E.M. from at least 10 measurements.

caused no further statistically significant change. The dose dependency of $I_{ci,in}$ was tested in the range of 0.1–20 mM (Fig. 1*C*). Even at the highest concentrations tested, the value of $I_{ci,in}$ was still increasing. Thus, the dose–response characteristics of $I_{ci,out}$ and $I_{ci,in}$ were different as regards both the size of the current ($I_{ci,out} \gg I_{ci,in}$), the threshold concentration ($I_{ci,out} \ll I_{ci,in}$) and the saturation level.

Enzyme-spectrophotometric measurements

Incubation of PC-3M cells with 10 mM citrate in the EB solution resulted in a $9.0 \pm 3.7\%$ increase in the intracellular citrate content, which was significant ($P = 0.041$; $n = 4$) (Fig. 2*A*; control (2) *versus* control (1)). Cells incubated with citrate in low-Na^+ EB solution did not show any significant increase in the amount of intracellular citrate ($P = 0.112$; $n = 4$). On the other hand, high-K^+ increased the amount of citrate uptake into the cells by $20.0 \pm 4.1\%$, which was significant ($P = 0.023$; $n = 4$) (Fig. 2*A*). Thus, uptake of citrate ($I_{ci,in}$) was dependent primarily upon Na^+; however, under conditions of reduced outward K^+ gradient, K^+-dependent uptake of citrate could be seen.

Release of citrate from pre-loaded PC-3M cells appeared variable and more difficult to detect (Fig. 2*B*). Under control and low-Na^+ conditions, very little citrate was released into the medium and its level rose only very slightly in time. In contrast, citrate release was reduced in high-K^+ medium (Fig. 2*B*).

The data from the enzyme-spectrophotometric measurements were consistent with the electrophysiology therefore in showing that citrate uptake and release were primarily Na^+ and K^+ dependent, respectively.

Ionic characteristics

The reversal potentials of $I_{ci,out}$ and $I_{ci,in}$ were determined by measuring the currents at different holding potentials (Fig. 3*A*). Thus, the following values were obtained: -1.0 ± 1.2 mV ($I_{ci,out}$) and -4.6 ± 1.3 mV ($I_{ci,in}$). The difference was statistically significant ($P = 0.021$; $n = 7$–8; Fig. 3*A*).

The ionic bases of $I_{ci,out}$ and $I_{ci,in}$ were elucidated by applying EB solutions with altered ionic content and measuring their effects. The same solutions were also tested under control conditions (i.e. with no citrate present) and then the pairs of effects were compared. Of the different ions (K^+, Na^+, Ca^{2+}, Cl^-, Mg^{2+}) tested, only K^+ produced a statistically significant effect on $I_{ci,out}$ (Fig. 3*B* and *C*). This effect was dose dependent and qualitatively the same for either 0.1 mM or 10 mM intracellular citrate. The slopes of the dependence of $I_{ci,out}$ on K^+ were similar: 34.0 and 39.2 pA per 10-fold change in $[K^+]_o$ for 0.1 and 10 mM intracellular citrate, respectively (Fig. 3*C*). The dependence of $I_{ci,out}$ on the *trans*-membrane K^+ concentration gradient was also seen by testing the intracellular effects of K^+- *versus* Na^+-citrate. Thus, $I_{ci,out}$ produced by application of K^+-citrate was $48.1 \pm 22.0\%$

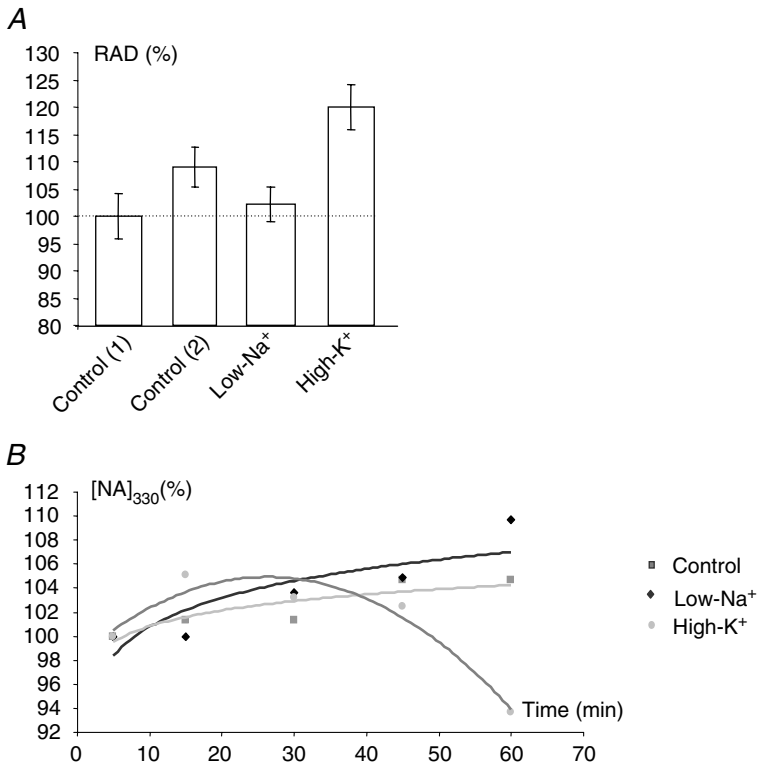

Figure 2. Spectrophotometric measurements from PC-3M cells of citrate uptake and release
A, uptake. RAD (%), relative absorbance difference (i.e. reading from EB solution alone subtracted from the solutions containing also cell digests) expressed relative to control EB solution containing digests of cells with no prior exposure to citrate (left-most histobar). The latter, Control (1), was treated as 100%. Other conditions were as follows: Control (2), EB solution containing the digests of cells pre-incubated in 10 mM Na^+-citrate for 30 min: Low-Na^+ citrate, same as Control (2) but in EB solution with reduced Na^+ (37.8 mM; equimolar choline used as the substitute): High-K^+, same as Control (2) but in EB solution with increased, 54 mM K^+ (equimolar Na^+ removed). Each histobar denotes mean ± S.E.M. ($n = 4$). *B*, spectrophotometric measurements (at 330 nm) of citrate release from PC-3M cells pre-incubated in 10 mM Na^+-citrate for 30 min. Time course and ionic dependence of citrate release are shown. The data are given as 'normalized absorption' ($[NA]_{330}$), i.e. individual experimental data are expressed relative to the first value (100%) measured at time = 5 min. Squares, control data, i.e. citrate release from cells into normal EB solution. Diamonds, citrate release into EB solution with reduced Na^+ (as in *A*). Circles, citrate release into EB solution with increased K^+ (as in *A*).

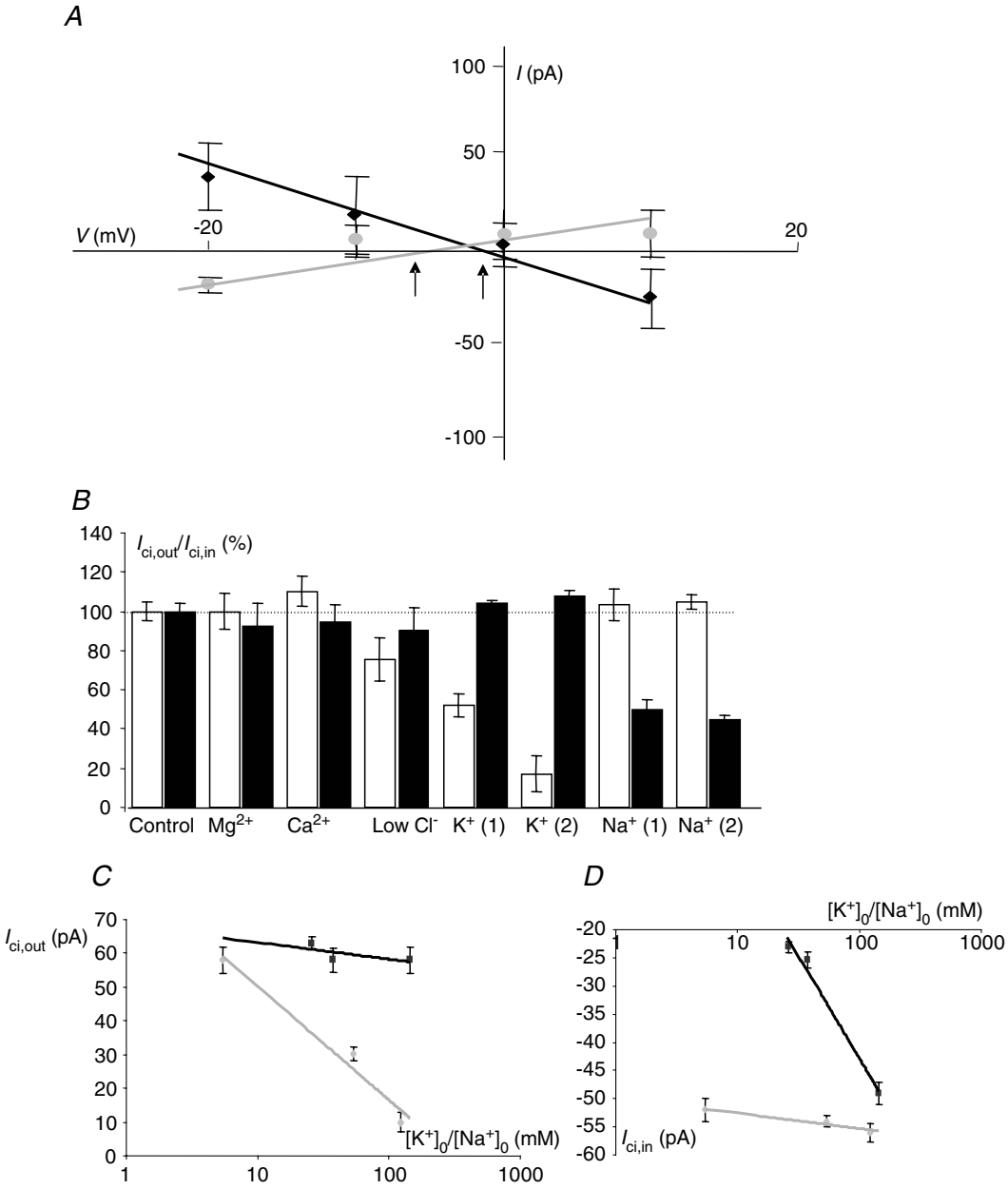

Figure 3. Ionic characteristics of $I_{ci,out}$ and $I_{ci,in}$

A, voltage dependence of membrane currents induced by 10 mM intracellular or extracellular citrate ($I_{ci,out}$ and $I_{ci,in}$ black squares and grey circles, respectively). In each case, 0.05 mM citrate was present on the opposite side. Arrows indicate the membrane reversal potential for $I_{ci,out}$ (right) and $I_{ci,in}$ (left). *B*, sensitivity of $I_{ci,out}$ and $I_{ci,in}$ to extracellular ions. The substitutes used for the different ions were as follows: Mg^{2+} (none or Ca^{2+}), Ca^{2+} (none or Mg^{2+}), Cl^- (gluconate), K^+ (Na^+) and Na^+ (choline). The data are presented as a percentage of the respective control currents (I_{cit} and $I_{cit,in}$) taken as 100%. K^+ (1) and K^+ (2) correspond to extracellular K^+ concentration ($[K^+]_o$) of 54 and 118 mM K^+. Na^+ (1) and Na^+ (2) denote 37.8 and 26 mM extracellular Na^+ concentration ($[Na^+]_o$), respectively. Only changes in $[K^+]_o$ had a significant effect on $I_{ci,out}$; in contrast, $I_{ci,in}$ was mainly affected by $[Na^+]_o$. Thus, increasing $[K^+]_o$ decreased $I_{ci,out}$ whilst decreasing $[Na^+]_o$ reduced $I_{ci,in}$, both in a dose-dependent manner. *C*, dependence of $I_{ci,out}$ $[K^+]_o$ (grey diamonds) and $[Na^+]_o$ (black squares) for the working concentration of (0.1 mM) intracellular Na^+-citrate. $[K^+]_o$ was increased from the normal value of 5.4 mM to 54 and 118 mM, whilst Na^+ was decreased from the normal value of 144 mM to 37.8 and 26 mM (plotted on a logarithmic scale). Each data point denotes mean ± S.E.M. ($n > 7$). Equimolar Na^+ was used as the K^+ substitute. *D*, as in *C* but for $I_{ci,in}$. Equimolar choline$^+$ was used as the Na^+ substitute.

bigger, compared with equimolar Na^+-citrate (Fig. 5*A*). The differences at the respective concentrations were statistically significant ($P = 0.0041$; $n = 8$–10).

In contrast, $I_{ci,in}$ had a different ionic dependence. The inward current was only weakly K^+ dependent and only when the extracellular K^+ concentration was increased. Thus, the current amplitudes recorded were -52.1 ± 0.9 pA (control) and -54.0 ± 1.2 pA (56 mM K^+) and these values were not significantly different ($P > 0.05$; $n = 7$–8). On the other hand, at the highest K^+ concentration used (118 mM) the value of $I_{ci,in}$ recorded (-56.4 ± 1.7 pA) was significantly greater than normal ($P = 0.04$; $n = 6$–7) (Fig. 3*B* and *D*). Importantly, $I_{ci,in}$ showed a strong Na^+ dependence, the value of $I_{ci,in}$ decreasing by some -49.3 pA for a 10-fold reduction in the extracellular Na^+ concentration (Fig. 3*D*).

Na^+ stoichiometry of inward citrate transporter

Assuming that the inward citrate current ($I_{ci,in}$) in normal EB solution was predominantly Na^+ dependent, the stochiometry could be determined as described before (Chen *et al.* 1998; Mycielska & Djamgoz, 2004). Accordingly, 5 and 10 mM Na^+-citrate salt solutions were applied extracellularly whilst the holding potential was varied in the range -45 to $+10$ mV (Fig. 4*A*). The shift in the reversal potential between 10 and 5 mM extracellular citrate application was 17.5 ± 0.1 mV ($n = 8$; Fig. 4*A*), giving a stoichiometry value of 4.0 ± 0.1. Thus, the inward transport of one trivalent citrate anion by the Na^+-dependent transporter would involve the co-transport of four Na^+, with a net inward current.

Tests of transporter *versus* possible anion channel characteristics

The possibility that $I_{ci,in}$ represented membrane currents through an anion channel was ruled out by two different types of experiment. First, possible differential effects of two Cl^- channels blockers (lonidamine and 9-AC) were tested on resting Cl^- conductance and $I_{ci,in}$ and $I_{ci,out}$ (Fig. 4*B*). Lonidamine and 9-AC (100 μM each) reduced the Cl^- currents by 30–40%, compared with the control value ($P < 0.001$; $n = 9$; Fig. 4*B*). However, the same drugs had no effect on the amplitudes of $I_{ci,in}$ or $I_{ci,out}$ (Fig. 4*B*). Second, in the case of $I_{ci,in}$, a further test could be performed. Thus, the voltage dependences of $I_{ci,in}$ induced by pulses of 5 or 10 mM extracellular citrate (with equimolar citrate present on the intracellular side) were linear with reversal potentials of -10.0 ± 1.3 and 4.0 ± 1.8 mV ($P = 0.012$; $n = 11$) (Fig. 4*C*). The shift in the reversal potential observed as well as the result of the Cl^- channel blocker experiments (Fig. 4*B*) are consistent with $I_{ci,in}$ and $I_{ci,out}$ having mainly transporter characteristics.

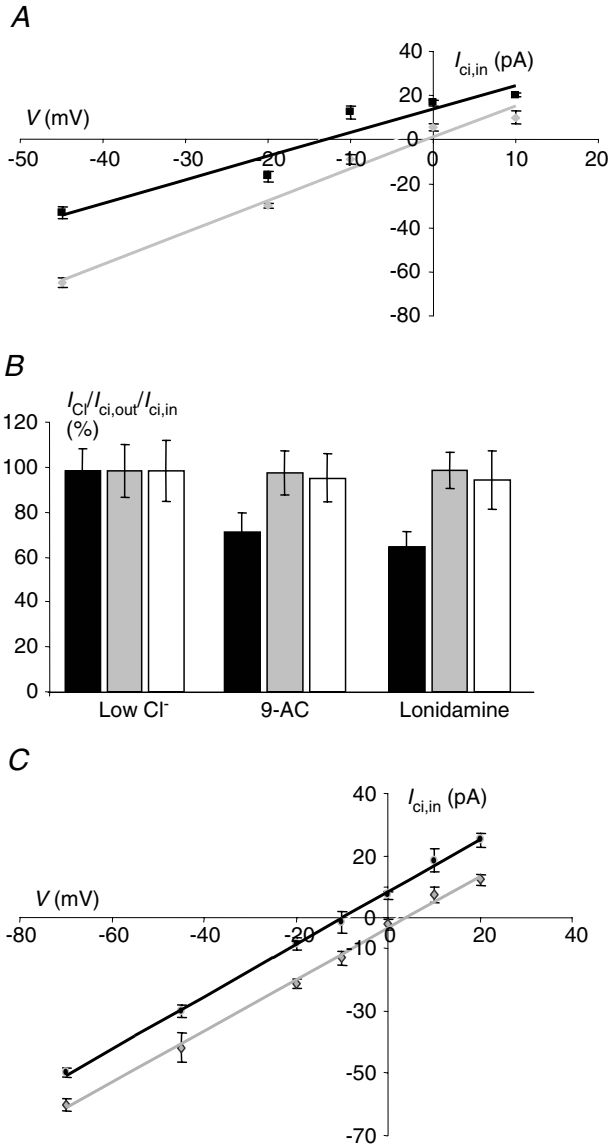

Figure 4. Transporter characteristics of $I_{ci,in}$
Current–voltage relationship of $I_{ci,in}$ for 5 and 10 mM extracellular Na^+-citrate (black squares and grey diamonds, respectively), with 0.05 mM intracellular Na^+-citrate present. These data show a shift in the reversal potential of 17.6 ± 1.1 mV. Each data point is the mean ± S.E.M. of 10 measurements. *B*, effects of anion channel blockers on Cl^- current (I_{Cl}) (elicited by reducing the extracellular Cl^- concentration 10-fold using equimolar gluconate as the substitute – black histobars), 0.1 mM intracellular Na^+-citrate ($I_{ci,out}$ – grey histobars) and 10 mM extracellular Na^+-citrate ($I_{ci,in}$ – white histobars). Currents were recorded under control conditions (left-most histobars) and in the presence of 9-AC (100 μM) and lonidamine (100 μM). Currents are expressed as a percentage of the control values treated as 100%. Each histobar represents the mean ± S.E.M. ($n \geq 7$). *C*, current–voltage relationship of $I_{ci,in}$ for two different concentrations of extracellular Na^+-citrate (5 and 10 mM – black squares and grey diamonds, respectively). These experiments were done under 'fixed-gradient' conditions (i.e. 5 and 10 mM intracellular citrate, respectively, present). Each data point denotes mean ± S.E.M. ($n \geq 6$).

Substrate specificity and inhibitor profiles

Intracellular application of Na^+ and K^+ salts of citrate and several other Krebs cycle intermediates (all at 0.1 mM) suggested the following order of potency for outward currents (Fig. 5*A*):

Citrate (K^+) > citrate (Na^+) = malate = succinate = isocitrate > NaCl.

On the other hand, application of extracellular 10 mM concentrations of the various different Krebs cycle intermediates suggested a different profile for the inward currents, as follows:

Citrate (K^+) = citrate (Na^+) > malate = succinate > isocitrate > NaCl.

It appeared therefore that there were significant differences between the potency orders of the substrates used. In particular, K^+-*versus* Na^+-citrate was more effective in generating outward currents (Fig. 5*A*).

The effects of several potential inhibitors on $I_{ci,in}$ and $I_{ci,out}$ were studied (Fig. 5*B*). Amiloride had qualitatively and quantitatively different effects, increasing $I_{ci,out}$ by 8% but decreasing $I_{ci,in}$ by 17% ($P = 0.043$ and $P = 0.024$ respecively; $n = 7$–8). Tetrodotoxin had the opposite effect, reducing $I_{ci,out}$ by 10% and increasing $I_{ci,in}$ by 28% ($P = 0.041$ and $P = 0.026$, respectively; $n = 8$–10). The effects of LiCl were qualitatively similar to amiloride, resulting in 26% increase of $I_{ci,out}$ and 10% decrease of $I_{ci,in}$ ($P = 0.002$ and $P = 0.041$, respectively; $n = 10$–11). 4-Aminopyridine had an inhibitory effect on both $I_{ci,out}$ (10%) and $I_{ci,in}$ (8%) ($P = 0.036$ and $P = 0.009$, respectively; $n = 10$–12). DEPC had a similar effect on $I_{ci,out}$ and $I_{ci,in}$ (17 and 12% reductions, $P = 0.007$ and $P = 0.039$, respectively; $n = 11$–13). The following agents had no net effect: ouabain (applied for 1 min), phloretin and SCH 28080.

It was concluded that the pharmacological profiles of $I_{ci,in}$ and $I_{ci,out}$ were qualitatively different.

pH sensitivities

The pH sensitivities of $I_{ci,in}$ and $I_{ci,out}$ were studied by changing intracellular pH (pH_i) and extracellular pH (pH_o) in separate experiments, as follows.

Extracellular pH. Acidifiying pH_o from 7.2 to 6.5 resulted in a slight outward current (13.1 ± 1.1 pA; $n = 10$) in the control condition (Fig. 6*A*). A similar reaction was recorded when intracellular citrate was present (17.0 ± 2.2 pA; $n = 9$). These values were not significantly different ($P > 0.05$). Opposite effects were seen by alkalization of pH_o to 8.0, i.e. inward currents of -15.0 ± 2.1 pA ($n = 7$) and -22.3 ± 3.1 pA ($n = 10$) were recorded with and without intracellular citrate; again, the difference was not significant ($P > 0.05$) (Fig. 6*A*). The same treatments (i.e. pH_o 7.2 to 6.5 and 7.2 to 8.0) also had no significant effect on $I_{ci,in}$ (Fig. 6*B*).

Intracellular pH. Acidifying pH_i under control recording conditions resulted in an inward current of -9.1 ± 2.1 pA ($n = 7$); this increased to -14.0 ± 1.9 ($n = 8$) when intracellular citrate was present. This change was significant ($P = 0.044$). Alkalization of pH_i resulted in outward currents which were similar under both control conditions

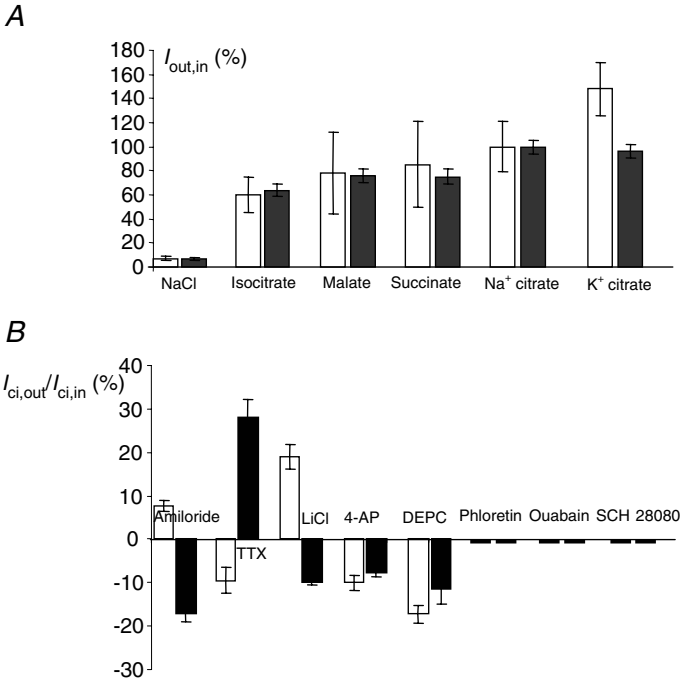

Figure 5. Substrate specificity and inhibitor profile of $I_{ci,out}$ and $I_{ci,in}$
A, substrate specificity of $I_{ci,out}$ (white bars) and $I_{ci,in}$ (black bars). The outward currents were generated by Na^+ and K^+ salts of citrate and a range of carboxylates at the working concentrations of 0.1 mM. The inward currents were generated by 10 mM Na^+ and K^+ salts of citrate and a range of carboxylates. Both currents are plotted as a percentage of the current generated by Na^+-citrate salt (considered to be 100%). Each histobar represent mean ± S.E.M. ($n \geq 10$). *B*, inhibitor-induced changes in $I_{ci,out}$ (generated by 0.1 mM Na^+-citrate; white histobars) and $I_{ci,in}$ (generated by 10 mM extracellular Na^+-citrate; black bars). Positive and negative values indicate increase and decrease in current, respectively, expressed as a percentage of the control (i.e. current measured with no citrate present). Each histobar represents mean ± S.E.M. ($n \geq 7$). The inhibitors (concentrations) used were as follows: amiloride (1 mM); TTX (1 μM); LiCl (10 mM); 4-AP (5 mM); DEPC (2 mM); phloretin (0.1 mM); ouabain (50 μM); SCH 28080 (50 μM).

and when intracellular citrate was present (22.7 ± 5.1 *versus* 20.1 ± 1.8 pA, respectively; $n = 7$–8; $P > 0.05$) (Fig. 6*C*). Changing pH_i also had no effect on $I_{ci,in}$ (Fig. 6*D*).

In conclusion, changing pH_o or pH_i in either direction had no effect on $I_{ci,in}$, i.e. uptake of citrate was not pH dependent. In contrast, the outward citrate current was pH_i sensitive being reduced by acidification, but not alkalization.

Tests of citrate transporter mRNA expression

Expression of known citrate transporter, NaDC1, NaDC1sv (alternative splice variant of NaDC1), NaDC3 and NaCT mRNAs in the PC-3M and the normal human prostatic epithelial PNT2-C2 cell lines were evaluated by reverse-transcription PCR (Fig. 7). In both prostate cell lines, no amplification product could be obtained thereby suggesting that NaDC1, NaDC1sv, NaDC3 and NaCT mRNAs were not expressed (Fig. 7*A*). In contrast, the same primers readily amplified PCR products of the expected size (200–203 bp) from kidney and liver cDNAs, used as positive controls. Thus, liver expressed NaDC3 and NaCT, whilst kidney expressed NaDC1 (Fig. 7*B*), as expected (Inoue *et al.* 2002). NaDC1sv was not expressed in either control tissue. In all cases, as an 'internal' control for the mRNA quality, the cDNAs prepared from the PNT2-C2 and PC-3M cell lines tested positive for β-actin (Fig. 7*B*).

Effects of Zn^{2+}

The effects of intracellular Zn^{2+} application as well as TPEN (a membrane-permeant Zn^{2+} chelator) were studied on PC-3M cells. TPEN (50 μM) had no effect on the holding current (not shown). On the other

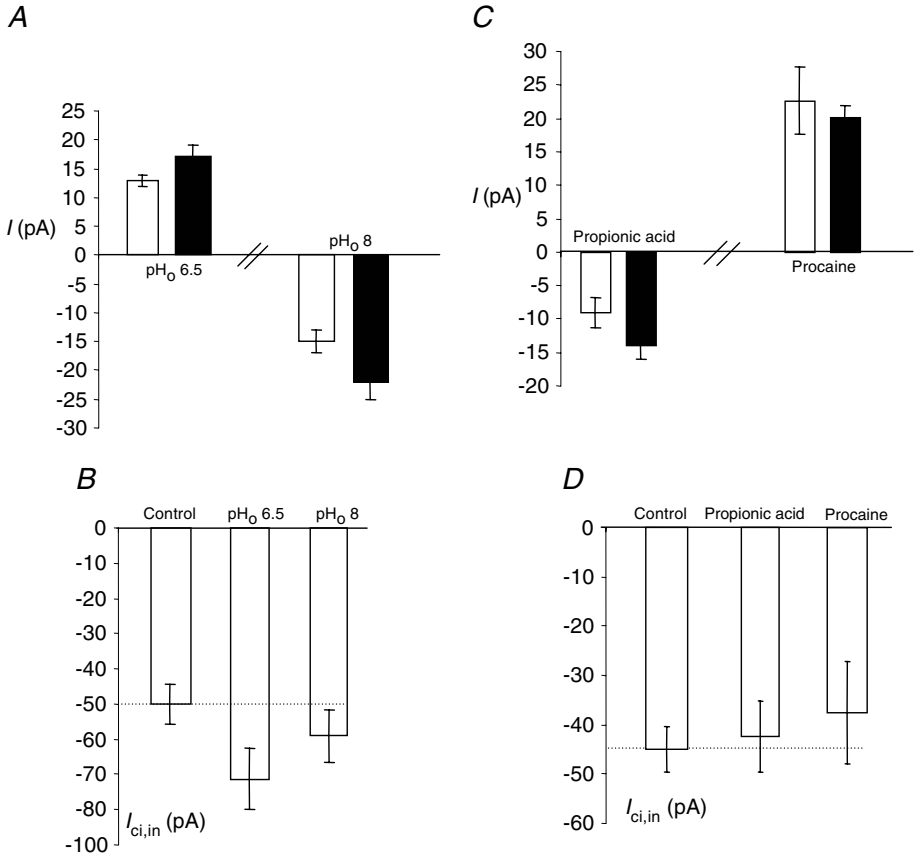

Figure 6. pH sensitivity of PC-3M cells: $I_{ci,in}$ and $I_{ci,out}$
A, membrane currents (*I*) recorded under control conditions (white bars) and with 0.1 mM intracellular Na^+-citrate present (black bars). Changing extracellular pH_o from the normal value of 7.2–6.5 or 8 had the same effect, i.e. $I_{ci,out}$ was not significantly affected by changes in extracellular pH. *B*, as in *A* but for $I_{ci,in}$. Again, there was no significant effect changing the extracellular pH. *C*, acidifying intracellular pH with propionic acid (30 mM) slightly but significantly decreased $I_{ci,out}$. On the other hand, intracellular alkalization with procaine (10 mM) had no effect. *D*, as in *C* but for $I_{ci,in}$. There was no effect of changing the intracellular pH on $I_{ci,in}$. Each histobar represents mean ± S.E.M. ($n \geq 7$).

hand, increasing the intracellular Zn^{2+} concentration by dialysing with 1 mM Zn^{2+} resulted in an outward current of 90.7 ± 18.4 pA ($n = 12$). The appearance of this current was noticeably delayed for about 90.8 ± 18.4 s ($n = 12$). There was considerable variability in both the value and latency of the Zn^{2+}-induced outward current.

Effects of long-term treatment with TTX

Since citrate and VGSC expression have both been associated with prostate cancer, we investigated whether blocking VGSC activity would affect citrate transport. Thus, PC-3M cells were pre-incubated with TTX (1 μM) for 24 or 48 h, and then $I_{ci,out}$ and $I_{ci,in}$ were measured. Following the TTX treatment, $I_{ci,out}$ became significantly increased: 58.2 ± 19.1 pA (control), 134.8 ± 31.2 pA (24 h) and 128.6 ± 19.0 pA (48 h) ($P = 0.001$ compared with control for both treatments; $n = 10$–12 for both) (Fig. 8*A*). In contrast, the same treatment caused a significant *decrease* in $I_{ci,in}$: -52.1 ± 5.3 pA (control), -30.3 ± 1.9 pA (24 h) and -18.0 ± 1.6 pA (48 h); $P < 0.001$ compared with control; $n = 18$ for both) (Fig. 8*B*).

We also investigated the effect of the TTX pre-treatment on the expression of Nav1.7, the TTX-sensitive VGSC isoform expressed predominantly in the closely related strongly metastatic PC-3 prostate cancer cell line (Diss *et al.* 2001). Nav1.7 mRNA was significantly up-regulated following TTX pre-treatment, by 2.2-fold (propagated standard error: +0.62, −0.41; $P < 0.001$; $n = 3$) after 24 h, and by 2.3-fold (propagated standard error: +0.94, −0.61; $P = 0.021$; $n = 3$) after 48 h (Fig. 8*C*).

The TTX incubation had no effect on the partial permeability of the membrane to Na^+ whilst there was a significant increase in K^+ permeability (Fig. 8*D*).

Ionic dependence of $I_{ci,out}$ was studied as before using different concentrations of extracellular K^+ and Na^+. As in the case of untreated cells, high-K^+ significantly and in a dose-dependent manner reduced $I_{ci,out}$ at both concentrations (54 and 118 mM) ($P = 0.037$–0.001; $n = 10$–15) (Figs 3*B* and *C*, and 9*A*). Similarly, as in the control case described above, reducing extracellular Na^+ did not cause any change in $I_{ci,out}$ in either low-Na^+ EB solution used (40.4 and 26 mM) (Figs 3*B* and *C*, and 9*B*). Thus, the overall ionic dependence of $I_{ci,out}$ did not change after long-term TTX pre-incubation.

Unlike control experiments, where high-K^+ EB solutions reduced $I_{ci,in}$ only slightly and at the highest concentration used (Fig. 3*B* and *D*), following TTX pre-incubation (24 and 48 h) the inward current induced by extracellular citrate became highly sensitive to change in the external K^+ concentration. Thus, application of high-K^+ EB solutions (containing 56 or 18 mM K^+) increased $I_{ci,in}$ significantly and in a dose-dependent manner ($P < 0.001$; $n = 11$–14) (Fig. 9*C*). On the other hand, following the TTX pre-incubation, low-Na^+ EB solution was mostly ineffective in reducing $I_{ci,in}$; the only statistically significant reduction (25%) was seen after 48 h pre-incubation for the lowest (26 mM) Na^+ concentration used ($P = 0.0015$; $n = 16$; Fig. 9*D*). It was

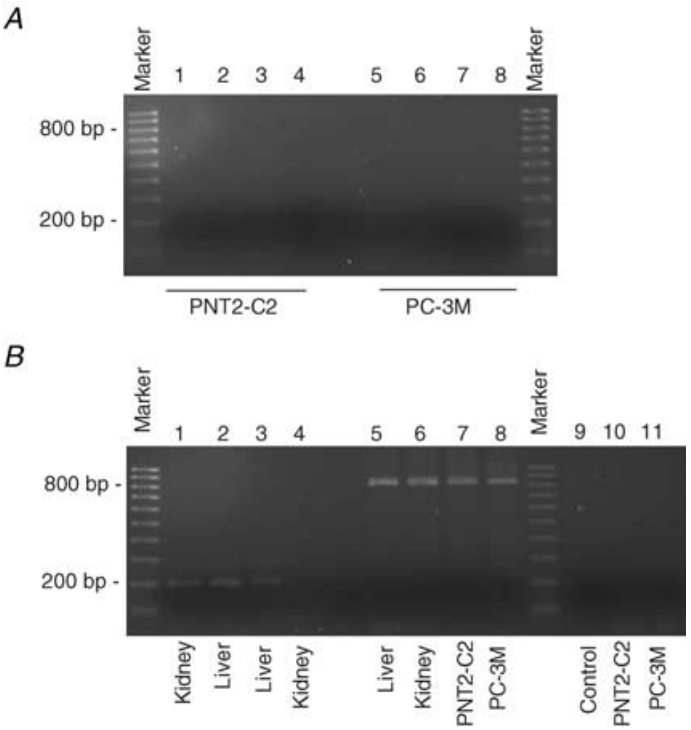

Figure 7. RT-PCR tests of known citrate transporter mRNA expression in prostate cell lines, PNT2-C2 and PC-3M
A, agarose gel electrophoresis of PCR reactions containing cDNA reverse-transcribed from RNAs prepared from PNT2-C2 cells and PC-3M cells using primers to known citrate transporters: NaDC1 (lanes 1 and 5), NaDC3 (lanes 2 and 6), NaCT (lanes 3 and 7) and NaDC1sv (lanes 4 and 8). *B*, further RT-PCRs on PNT2-C2 cell, PC-3M cell and human kidney and liver tissue cDNAs (as indicated lower-most). Lane 1, NaDC1; lane 2, NaDC3; lane 3, NaCT; lane 4, NaDC1sv. Lanes 5–8, control PCR reactions for β-actin with the different cell/tissue cDNAs, showing successful amplification of the expected band at 838 bp. Lane 9, negative control RT-PCR (no cDNA present). Lanes 10 and 11, negative controls for genomic contamination (PNT2-C2 and PC-3M cell mRNAs, respectively). Molecular markers used were in the range from 100 bp to 1000 bp, in 100 bp increments, and are indicated on the left (in both *A* and *B*).

concluded that $I_{ci,in}$ (i.e. citrate uptake), which was predominantly Na^+ dependent, became strongly K^+ sensitive whilst the Na^+-dependent component of $I_{ci,in}$ disappeared (Fig. 9*E*).

Discussion

Electrophysiological characteristics

We adopted the PC-3M cell line as a model to study the characteristics of citrate transport in metastatic human prostate cancer, and compared these with analogous data obtained previously from the 'normal' prostatic epithelial PNT2-C2 cells (Mycielska & Djamgoz, 2004). These two cell types differed in their electrophysiological characteristics. In particular, PC-3M cells had a more negative membrane potential and resting permeability to Na^+, as well as K^+. The Na^+ permeability was TTX sensitive and probably corresponded to the background VGSC activity known to occur in metastatic human prostate cancer cells (Laniado *et al.* 1997).

Comparison of $I_{ci,out}$ and $I_{ci,in}$

The essential electrophysiological characteristics of the outward and inward membrane currents generated by intracellular and extracellular application of citrate, $I_{ci,out}$ and $I_{ci,in}$, respectively, were markedly different,

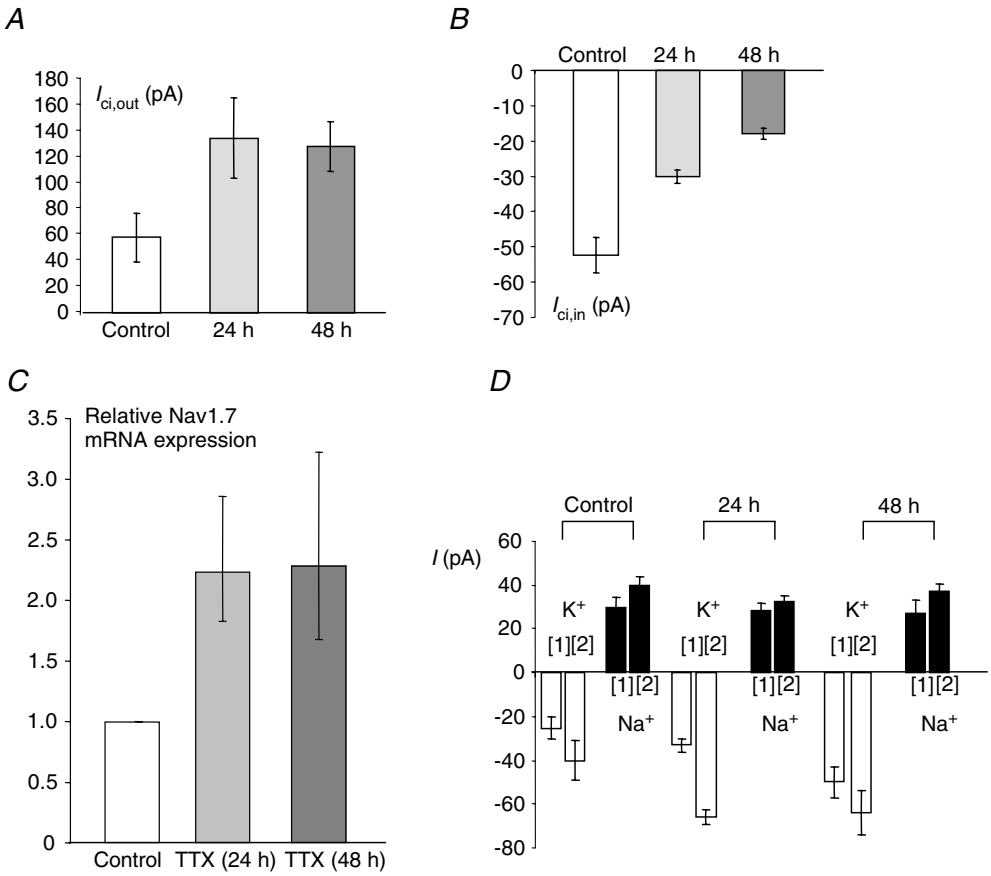

Figure 8. Effects of long-term pre-incubation with TTX
In *A*–*C*, control data are indicated by the white histobars, whilst the data obtained after 24 and 48 h of pre-treatment with TTX (1 μM) are shown as light and dark grey bars, respectively. Each histobar denotes mean ± S.E.M. ($n = 3$–7 independent treatments). *A*, $I_{ci,out}$ induced by 0.1 mM intracellular Na^+-citrate. *B*, $I_{ci,in}$ induced by 10 mM extracellular Na^+-citrate. *C*, Nav1.7 mRNA expression normalized to β-actin by the $2^{-\Delta\Delta Ct}$ method. *D*, membrane currents induced by increasing extracellular concentration to 54 mM [1] or 118 mM [2] or by lowering extracellular concentration to 37.8 mM [1] or 26 mM [2]. Thus, histobars indicate partial membrane permeabilities for Na^+ (black bars) and K^+ (white bars) in control conditions and after 24 and 48 h of 1 μM TTX pre-incubation. The data show that Na^+ permeability was not affected in the long-term presence of TTX whilst K^+ was increased. Na^+ was compensated in the K^+ substitutions. Choline was used as the substitute for Na^+. In *A*, *B* and *D*, each histobar denotes mean ± S.E.M. ($n \geq 10$). In *C*, error bars show errors propagated through the $2^{-\Delta\Delta Ct}$ analysis ($n = 3$).

as summarized in Table 1. The dose–response characteristics (Fig. 1*C*), substrate specificities (Fig. 5*A*) and pharmacological profiles (Fig. 5*B*) were also different. The basic difference in the ionic dependence of the two transporters was also seen in the enzyme spectrophotometric measurements (Fig. 2). Recent evidence suggests that significant changes occur in other Krebs cycle (monocarboxylate) transporters in malignancy (Miyauchi *et al.* 2004; Coady *et al.* 2004). Taken together, our results would suggest that PC-3M

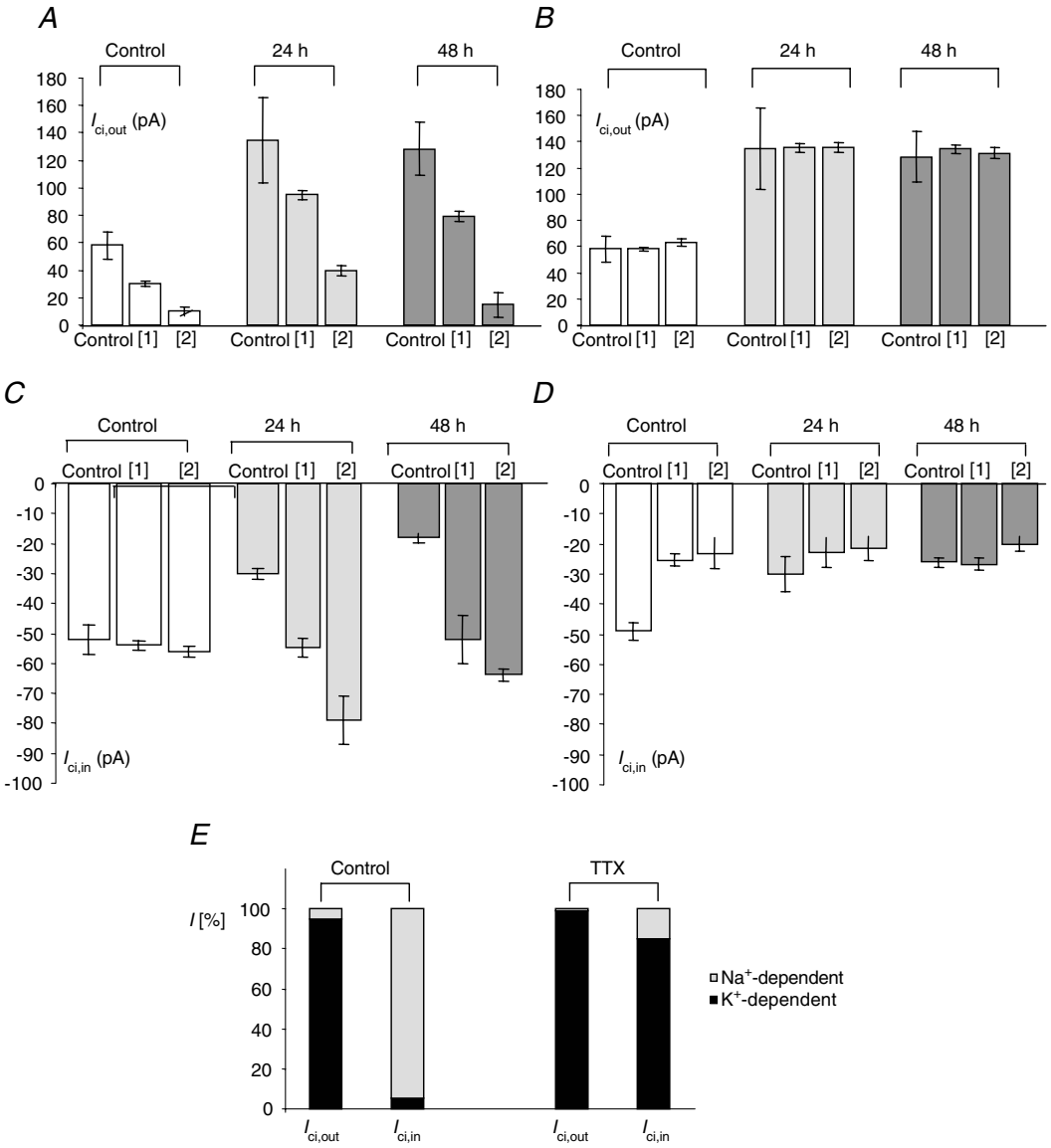

Figure 9. Effects of TTX pre-treatment on amplitude and ionic dependence of $I_{ci,out}$ and $I_{ci,in}$
A, K^+ dependence of $I_{ci,out}$ in control conditions (white bars), after 24 h (light grey bars) and 48 h (dark grey bars) of 1 μM TTX pre-incubation. [1] and [2] correspond to increase of extracellular K^+ concentration ($[K^+]_o$) to 54 and 118 mM K^+, respectively. *B*, Na^+ dependence of $I_{ci,out}$ in control conditions (white bars), after 24 h (light grey bars) and 48 h (dark grey bars) of 1 μM TTX pre-incubation. [1] and [2] correspond to reduction of extracellular Na^+ concentration ($[Na^+]_o$) to 37.8 and 26 mM Na^+, respectively. In all experiments, NaCl was replaced with equimolar choline chloride. *C*, K^+ dependence of $I_{ci,in}$ in control conditions (white bars), after 24 h (light grey bars) and 48 h (dark grey bars) of 1 μM TTX pre-incubation. [1] and [2] correspond to increase of $[K^+]_o$ to 54 and 118 mM, respectively. *D*, Na^+ dependence of $I_{ci,in}$ in control conditions (white bars), after 24 h (light grey bars) and 48 h (dark grey bars) of 1 μM TTX pre-incubation. [1] and [2] correspond to reduction of $[Na^+]_o$ to 37.8 and 26 mM, respectively. In all experiments NaCl was replaced with an equimolar concentration of choline chloride. Each histobar denotes mean ± S.E.M. ($n > 10$). *E,* summary of the data shown in *A–D* for $I_{ci,in}$ and $I_{ci,out}$, demonstrating the approximate percentage K^+- and Na^+-dependent components (dark and light parts of histobars) under control conditions (left-hand pair) and following treatment with 1 μM TTX for 48 h (right-hand pair).

Table 1. Comparison of basic characteristics of I_{cit}, $I_{ci,out}$ and $I_{ci,in}$ measured from PNT2-C2 (normal prostate) and PC-3M cells (prostate cancer)

Characteristic	Normal prostate	Prostate cancer	
	I_{cit}	$I_{ci,out}$	$I_{ci,in}$
Reversal potential	-1.0 ± 1.2 mV	0.7 ± 1.2 mV	-4.6 ± 1.3 mV
K^+ dependence	34.4 pA	34.0 pA	Not dependent
Na^+ dependence	Not dependent	Not dependent	36.5 pA
Alkalization	Not dependent	Not dependent	Not dependent
Acidification	Decrease	Decrease	Not dependent

Comparison of reversal potential, ionic (K^+ and Na^+) dependence and pH sensitivity of I_{cit}, $I_{ci,out}$ and $I_{ci,in}$. K^+ and Na^+ dependences are given as slopes for 10-fold change in extracellular concentrations. I_{cit} data are from Mycielska & Djamgoz (2004).

cells possess two different citrate transporters, a Na^+-dependent transporter primarily for uptake and a K^+-dependent efflux mechanism – this is the focus of the discussion that follows.

Characteristics and possible identity of $I_{ci,out}$

Several characteristics of $I_{ci,out}$ were similar to the current (I_{cit}) generated by outward citrate transport in PNT2-C2 cells (Mycielska & Djamgoz, 2004) (Table 1). In particular, the two currents have the same (i) reversal potential, (ii) K^+ dependence with almost identical slopes, (iii) Na^+ independence and (iv) preference for the trivalent form of citrate as inferred from pH sensitivity (Mycielska & Djamgoz, 2004). The substrate specificities were also very similar, as follows:

$I_{ci,out}$: K^+-citrate > malate = succinate > isocitrate (Fig. 5*A*);

I_{cit}: K^+-citrate > succinate = malate > isocitrate (Mycielska & Djamgoz, 2004). The slight difference could be due to some 'contamination' from the inward transporter. The differences in sensitivities to TTX, amiloride and phloretin are more likely to reflect the presence/absence of associated ionic regulatory mechanisms (Mycielska & Djamgoz, 2004).

In conclusion, $I_{ci,out}$ and I_{cit} probably represent the same K^+-dependent citrate mechanism (normally functioning outward) that we characterized earlier in the normal human prostate epithelial PNT2-C2 cell line (Mycielska & Djamgoz, 2004).

Characteristics and possible identity of $I_{ci,in}$

The citrate uptake current ($I_{ci,in}$) was consistent with transporter rather than ion channel activity (Fig. 4*C*), as in the case of I_{cit} (Mycielska & Djamgoz, 2004). Accordingly, DEPC which binds histidine and is known to partially inhibit most of the known tri/Gdicarboxylates transporters was effective in reducing $I_{ci,out}$ and $I_{ci,in}$ within the same range. However, many other characteristics of $I_{ci,in}$ were very different from $I_{ci,out}/I_{cit}$. Importantly, $I_{ci,in}$ was primarily Na^+ dependent, also reflected by the sensitivity to amiloride and TTX (blockers of Na^+ channels that may facilitate short-term recycling of Na^+ associated with the transporter).

Although the transporter was most specific for citrate, other Krebs cycle intermediates including succinate and malate were also carried. Stoichiometric measurements suggested that one citrate^{3-} was transported with four Na^+ into the cell. Changes in pH did not affect citrate inward current, which could be due to at least two different reasons. First, pH regulation in PC-3M, as a cancer cell line, may be different from normal (e.g. Izumi *et al.* 2003). This would seem unlikely, however, since the effects of changing pH were the same on the outward currents in both normal and cancer cells (Table 1). Second, and more likely, PC-3M cells possess an inward dicarboxylate transporter that would become apparent at acidified pH_o (when citrate becomes mainly divalent) and compensate for the reduced activity of the inward citrate transporter.

Taking the available evidence together, we would suggest that the transporter(s) representing $I_{ci,in}$ is designed primarily to carry citrate into the cell. This transporter has some similarity to previously characterized Na^+-dependent mainly 'inward' citrate/dicarboxylate transporters. The $I_{ci,in}$ transporter resembles NaCT (Inoue *et al.* 2002) as regards citrate specificity (preference for the high affinity form of the trivalent form of citrate) and Na^+ dependence/stoichiometry. However, unlike NaCT (but similar to NaDC1/3 transporters), $I_{ci,in}$ was suppressed by Li^+ and not significantly affected by pH (Pajor, 1999; Inoue *et al.* 2003). The PCR data suggested that the citrate/dicarboxylate transporter(s) expressed in the two human prostate cell lines may be different from the known NaDC1, NaDC2 and NaCT. Further work is required to elucidate the molecular nature of the prostatic transporters.

Regulation of citrate transport in PC-3M cells by VGSC activity

PC-3M cells at rest had TTX-sensitive permeability to Na^+, consistent with expression of functional VGSCs, as already demonstrated for other strongly metastatic prostate cancer

lines (Grimes *et al.* 1995; Laniado *et al.* 1997; Smith *et al.* 1998). It has also been established that VGSC expression/activity plays an important role in the cells' metastatic behaviour (e.g. Djamgoz *et al.* 2001; Mycielska *et al.* 2003; Fraser *et al.* 2003). Since citrate metabolism is also intimately associated with prostate cancer, we questioned whether VGSC activity would affect citrate transport in PC-3M cells. Suppressing VGSC activity by TTX produced both short- and long-term effect on citrate transport in PC-3M cells.

Short-term effects. Applying TTX to cells, just before citrate, increased $I_{ci,in}$ but reduced $I_{ci,out}$ (Fig. 5*B*). This can most readily be explained by assuming that TTX-induced outward current/membrane hyperpolarization would increase the activity of the electrogenic (depolarizing) inward citrate transporter. This effect can also conversely explain the inhibitory effect of TTX pre-treatment on $I_{ci,out}$.

Long-term effects. Treatment of PC-3M cells with TTX for 24–48 h, had the opposite effect on $I_{ci,in}$ and $I_{ci,out}$. Thus, $I_{ci,in}$ (strictly, its Na^+ dependence) was almost completely abolished, inward citrate transport becoming strongly K^+ dependent (Fig. 9*E*). On the other hand, TTX pre-treatment only had a quantitative effect on $I_{ci,out}$, significantly increasing the current amplitude but not changing its ionic dependence (Fig. 9*E*). Thus, after the long-term TTX treatment, citrate transport in PC-3M cells behaved more like that in PNT2-C2 cells (Mycielska & Djamgoz, 2004).

At present, the precise mechanism(s) whereby VGSC activity could regulate $I_{ci,in}$ transporter in the long term is not known. However, two main possibilities may be considered: (1) *Indirect*. Since short-term blockage of VGSC activity (by TTX) had a significant (potentiating) effect upon $I_{ci,in}$ (Fig. 5*B*), one possibility is that the long-term effect of TTX treatment is mediated by a change in VGSC expression. There is indeed some evidence that VGSC activity can influence VGSC expression/activity (e.g. Dave *et al.* 2003; Aptowicz *et al.* 2004). In the present study, long-term TTX treatment (i) up-regulated the expression of the main VGSC subtype (Nav1.7) in PC-3M cells but (ii) did not affect the partial Na^+ permeability of the cells (Fig. 8*D*). However, the slight depolarization of the membrane potential that may result from these changes would not be likely to suppress $I_{ci,in}$ completely; (2) *Direct*. It is possible that suppressing VGSC activity caused down-regulation of the Na^+-dependent inward citrate transporter itself. VGSC activity is known to control the expression of other Na^+-dependent transporters, such as Na^+/K^+-ATPase (Mata *et al.* 1992; Yamamoto *et al.* 1994) and Na^+–Ca^{2+} exchanger (Craner *et al.* 2004). An interesting possibility is whether $I_{ci,in}$ represents the activity of a splice variant of the 'normal' K^+-dependent citrate transporter. If so, a change in membrane potential itself may induce a change in the selectivity of splice variant expression (Xie & Black, 2001) and thus the Na^+/K^+ dependency of the citrate transporter(s). Further work, including molecular cloning, is required to elucidate these possibilities.

Citrate transport in prostate cancer

Prostate gland is known to release large amounts of citrate and this would account for the very high level of citrate detected in prostatic fluid of normal men (Costello & Franklin, 2000). Concentration of K^+ in prostatic fluid (~65 mM; Kavanagh, 1985) is some 10-fold higher than in blood (~4 mM, e.g. Overgaard *et al.* 2002), consistent with K^+ normally being co-released with citrate. Concurrently, the level of Cl^- is low, since the high concentration of trivalent citrate anions would necessitate removal of Cl^- from prostatic fluid. It was indeed suggested that several different types of Cl^- channel found in prostatic epithelial cells would be involved in the removal of Cl^- from prostatic fluid (Kim *et al.* 2003) and the PC-3M cells also had basal Cl^- permeability. Prostatic citrate metabolism and transport change dramatically in cancer, and in metastatic disease, citrate levels become as low as those detected in other body fluids (Costello *et al.* 1999*b*). It has been suggested therefore that citrate *metabolism* and/or *transport* alter significantly during the metastatic process.

Metabolism. It was shown previously that PNT2-C2 cells were sensitive to intracellular Zn^{2+} (exogeneous and endogenous), indicative of tonic activity of m-aconitase (Liang *et al.* 1999; Mycielska & Djamgoz, 2004). Elevation of the intracellular Zn^{2+} in the PC-3M cells produced a similar but 2-fold greater effect, consistent with reduced intracellular Zn^{2+} and lack of effect of the Zn^{2+} chelator. These results agree with the observations of Costello & Franklin (1998) that intracellular Zn^{2+} is reduced significantly and, consequently, that there is higher level of activity of m-aconitase in prostate cancer cells. In turn, these effects may relate to changes in expression/activity of Zn^{2+} transporter(s) in prostate (Costello *et al.* 1999*b*).

Transport. Normal prostate cells exhibit a citrate : isocitrate ratio of 30–40 : 1, due to the rate-limiting m-aconitase (Costello *et al.* 2000*a*) and efflux of citrate occurs via a K^+-dependent transporter (Mycielska & Djamgoz, 2004). The situation in prostate cancer cells is not known but assuming that it would be similar to non-prostate 'normal' cells, a reduced citrate : isocitrate ratio of 10–11 : 1 may be expected when citrate non-oxidizing prostatic cells become oxidative (Costello *et al.* 2000*b*). This is accompanied by the additional

expression of a citrate uptake transporter, driven naturally by the transmembrane inward Na^+ concentration gradient. Thus, in metastatic human prostate epithelial PC-3M cells, citrate transport was both Na^+ and K^+ dependent and its inhibitor profile was more complex than in the case of normal PNT2-C2 cells. The effectiveness of the various ion channel blockers (e.g. TTX, amiloride, 4-AP) used would suggest that the ionic fluxes accompanying citrate transport may be recycled in an integrated system.

Overview and concluding remarks

Our overall conclusion is that citrate transport (and, probably, metabolism) in metastatic prostate cancer (exemplified here by the PC-3M cell line) is qualitatively and quantitatively different from normal (exemplified by the PNT2-C2 cells; Mycielska & Djamgoz, 2004). In particular, PC-3M cells express an additional Na^+-dependent citrate transporter, primarily for uptake, in close parallel with the pathophysiology of citrate in metastatic prostate cancer (Costello & Franklin, 2000). The K^+-dependent component appeared identical to the 'normal' transporter characterized earlier (Mycielska & Djamgoz, 2004). The inhibitor and pH sensitivities suggested that the Na^+-sensitive citrate transporter is also likely to be novel. Accordingly, mRNAs for the known transporters were not found in either prostatic cell line. Interestingly, expression of the Na^+-dependent citrate transporter was controlled by VGSC activity which we have suggested previously to accelerate metastatic prostate cancer (Djamgoz, 1998), by potentiating a range of cellular behaviours involved in the metastatic cascade, e.g. motility (Djamgoz *et al.* 2001; Fraser *et al.* 2003), endocytic membrane activity (Mycielska *et al.* 2003; Krasowska *et al.* 2004) and invasion (Grimes *et al.* 1995; Laniado *et al.* 1997; Smith *et al.* 1998). It will be interesting, in future work, to determine the molecular characteristics and physiology of the prostatic citrate transporters, mechanisms of their regulation and contribution to metastatic disease, including the interplay with VGSC expression/activity.

References

Aptowicz CO, Kunkler PE & Kraig RP (2004). Homeostatic plasticity in hippocampal slice cultures involves changes in voltage-gated Na^+ channel expression. *Brain Res* **998**, 155–163.

Chen X-Z, Shayakul C, Berger UV, Tian W & Hediger MA (1998). Characterization of a rat Na^+-dicarboxylate cotransporter. *J Biol Chem* **273**, 20972–20981.

Chu LW, Pettaway CA & Liang JC (2001). Genetic abnormalities specifically associated with varying metastatic potential of prostate cancer cell lines as detected by comparative genomic hybridization. *Cancer Genet Cytogenet* **127**, 161–167.

Coady MJ, Chang MH, Charron FM, Plata C, Wallendorff B, Sah JF, Markowitz SD, Romero MF & Lapointe JY (2004). The human tumour suppressor gene SLC5A8 expresses a Na^+-monocarboxylate cotransporter. *J Physiol* **557**, 719–731.

Costello LC & Franklin RB (1991). Concepts of citrate production and secretion by prostate. 1. Metabolic relationships. *Prostate* **18**, 25–46.

Costello LC & Franklin RB (1998). Novel role of zinc in the regulation of prostate citrate metabolism and its implications in prostate cancer. *Prostate* **35**, 285–296.

Costello LC & Franklin RB (2000). The intermediary metabolism of the prostate: a key to understanding the pathogenesis and progression of prostate malignancy. *Oncology* **59**, 269–282.

Costello LC, Franklin RB, Liu Y & Kennedy MC (2000*a*). Zinc causes a shift toward citrate at equilibrium of the m-aconitase reaction of prostate mitochondria. *J Inorg Biochem* **78**, 161–165.

Costello LC, Franklin RB & Narayan P (1999*a*). Citrate in the diagnosis of prostate cancer. *Prostate* **38**, 237–245.

Costello LC, Liu Y, Zou J & Franklin RB (1999*b*). Evidence for a zinc uptake transporter in human prostate cancer cells which is regulated by prolactin and testosterone. *J Biol Chem* **274**, 17499–17504.

Costello LC, Liu Y, Zou J & Franklin RB (2000*b*). Mitochondrial aconitase gene expression is regulated by testosterone and prolactin in prostate epithelial cells. *Prostate* **42**, 196–202.

Craner MJ, Newcombe J, Black JA, Hartle C, Cuzner ML & Waxman SG (2004). Molecular changes in neurons in multiple sclerosis: altered axonal expression of Nav1.2 and Nav1.6 sodium channels and Na^+/Ca^{2+} exchanger. *Proc Natl Acad Sci U S A* **101**, 8168–8173.

Dave JR, Yao C, Moffett JR, Berti R, Koeing M & Tortella FC (2003). Down regulation of sodium channel Na(v)1.1 expression by veratridine and its reversal by a novel sodium channel blocker, RS100642, in primary neuronal cultures. *Neurotox Res* **5**, 213–220.

Diss JK, Archer SN, Hirano J, Fraser SP & Djamgoz MB (2001). Expression profiles of voltage-gated Na^+ channel alpha-subunit genes in rat and human prostate cancer cell lines. *Prostate* **48**, 165–178.

Djamgoz MBA (1998). Voltage-gated sodium channel activity and metastasis: a novel approach to understanding the pathophysiology of prostate cancer. *J Physiol* **513*P***, 21–22*S*.

Djamgoz MBA, Mycielska M, Madeja Z, Fraser SP & Korohoda W (2001). Directional movement of rat prostate cancer cells in direct-current electric field: involvement of voltage gated Na^+ channel activity. *J Cell Sci* **114**, 2697–2705.

Feng P, Li TL, Guan ZX, Franklin RB & Costello LC (2003). Effect of zinc on prostatic tumorigenicity in nude mice. *Ann N Y Acad Sci* **1010**, 316–320.

Franklin RB, Ma J, Zou J, Kukoyi BI, Feng P & Costello LC (2003). Human ZIP1 is a major zinc uptake transporter for the accumulation of zinc in prostate cells. *J Inorg Biochem* **96**, 435–442.

Fraser SP, Salvador V, Manning EA, Mizal J, Altun S, Raza M, Berridge RJ & Djamgoz MB (2003*a*). Contribution of functional voltage-gated Na^+ channel expression to cell behaviors involved in the metastatic cascade in rat prostate cancer. I. Lateral motility. *J Cell Physiol* **195**, 479–487.

Grimes JA, Fraser SP, Stephens GJ, Downing JE, Laniado ME, Foster CS, Abel PD & Djamgoz MB (1995). Differential expression of voltage-activated Na^+ currents in two prostatic tumour cell lines: contribution to invasiveness in vitro. *FEBS Lett* **369**, 290–294.

Inoue K, Zhuang L, Maddox DM, Smith SB & Ganapathy V (2002). Structure, function, and expression pattern of a novel sodium-coupled citrate transporter (NaCT) cloned from mammalian brain. *J Biol Chem* **277**, 39469–39476.

Inoue K, Zhuang L, Maddox DM, Smith SB & Ganapathy V (2003). Human sodium-coupled citrate transporter, the orthologue of Drosophila Indy, as a novel target for lithium action. *Biochem J* **374**, 21–26.

Izumi H, Torigoe T, Ishiguchi H, Uramoto H, Yoshida Y, Tanabe M, Ise T, Musakami T, Yoshida T, Nomoto M & Kohno K (2003). Cellular pH regulators: potentially promising molecular targets for cancer chemotherapy. *Cancer Treat Rev* **29**, 541–549.

Kavanagh JP (1985). Sodium, potassium, calcium, magnesium, zinc, citrate and chloride content of human prostatic and seminal fluid. *J Reprod Fertil* **75**, 35–41.

Kim SJ, Shin SY, Lee JE, Kim JH & Uhm DY (2003). Ca^{2+}-activated Cl^- channel currents in rat ventral prostate epithelial cells. *Prostate* **55**, 118–127.

Krasowska M, Grzywna ZJ, Mycielska ME & Djamgoz MB (2004). Patterning of endocytic vesicles and its control by voltage-gated Na^+ channel activity in rat prostate cancer cells: fractal analyses. *Eur Biophys J* **33**, 535–542.

Kreuzer KA, Lass U, Landt O, Nitsche A, Laser J, Ellerbrok H, Pauli G, Huhn D & Schmidt CA (1999). Highly sensitive and specific fluorescence reverse transcription-PCR assay for the pseudogene-free detection of beta-actin transcripts as quantitative reference. *Clin Chem* **45**, 297–300.

Laniado ME, Lalani EN, Fraser SP, Grimes JA, Bhangal G, Djamgoz MB & Abel PD (1997). Expression and functional analysis of voltage-activated Na^+ channels in human prostate cancer cell lines and their contribution to invasion in vitro. *Am J Pathol* **150**, 1213–1221.

Li H, Myeroff L, Smiraglia D, Romero MF, Pretlow TP, Kasturi L, Lutterbaugh J, Rerko RM, Casey G, Issa JP, Willis J, Willson JK, Plass C & Markowitz SD (2003). SLC5A8, a sodium transporter, is a tumor suppressor gene silenced by methylation in human colon aberrant crypt foci and cancers. *Proc Natl Acad Sci U S A* **100**, 8412–8417.

Liang JY, Liu YY, Franklin RB, Costello LC & Feng P (1999). Inhibitory effect of zinc on human prostatic carcinoma cell growth. *Prostate* **40**, 200–207.

Livak KJ & Schmittgen TD (2001). Analysis of relative gene expression data using real-time quantitative PCR and the 2(-Delta Delta C(T) Method. *Methods* **25**, 402–408.

Mata M, Hieber V, Beaty M, Clevenger M & Fink DJ (1992). Activity-dependent regulation of Na^+,K^+-ATPase alpha isoform mRNA expression in vivo. *J Neurochem* **59**, 622–626.

Miyauchi S, Gopal E, Fei YJ & Ganapathy V (2004). Functional identification of SLC5A8, a tumor suppressor down-regulated in colon cancer, as a Na^+-coupled transporter for short-chain fatty acids. *J Biol Chem* **279**, 13293–13296.

Mycielska ME & Djamgoz MBA (2004). Citrate transport in the human prostate epithelial PNT2-C2 cell line: Electrophysiological analyses. *J Physiol* **559**, 821–833.

Mycielska ME, Fraser SP, Szatkowski M & Djamgoz MB (2003). Contribution of functional voltage-gated Na^+ channel expression to cell behaviors involved in the metastatic cascade in rat prostate cancer. II. Secretory membrane activity. *J Cell Physiol* **195**, 461–469.

Overgaard K, Lindstrom T, Ingemann-Hansen T & Clausen T (2002). Membrane leakage and increased content of Na^+-K^+ pumps and Ca^{2+} in human muscle after a 100-km run. *J Appl Physiol* **92**, 1891–1898.

Pajor AM (1999). Sodium-coupled transporters for Krebs cycle intermediates. *Annu Rev Physiol* **61**, 663–682.

Petrarulo M, Facchini P, Cerelli E, Marangella M & Linari F (1995). Citrate in urine determined with a new citrate lyase method. *Clin Chem* **41**, 1518–1521.

Smith P, Rhodes NP, Shortland AP, Fraser SP, Djamgoz MB, Ke Y & Foster CS (1998). Sodium channel protein expression enhances the invasiveness of rat and human prostate cancer cells. *FEBS Lett* **423**, 19–24.

Xie J & Black DL (2001). A CaMK IV responsive RNA element mediates depolarization-induced alternative splicing of ion channels. *Nature* **410**, 936–939.

Yamamoto K, Ikeda U, Okada K, Saito T, Kawakami K & Shimada K (1994). Sodium ion mediated regulation of Na/K-ATPase gene expression in vascular smooth muscle cells. *Cardiovasc Res* **28**, 957–962.

Acknowledgements

This study was supported by a project grant from The Wellcome Trust and the Pro Cancer Research Fund (PCRF).